

Biquadratic and Quadratic Springs for Modeling St Venant Kirchhoff Materials

Hervé Delingette

ASCLEPIOS Research Project
INRIA Sophia-Antipolis, 2004 route des Lucioles
06902 Sophia-Antipolis, France

Abstract. This paper provides a formal connexion between springs and continuum mechanics in the context of two-dimensional and three dimensional hyperelasticity. First, we establish the equivalence between surface and volumetric St Venant-Kirchhoff materials defined on linear triangles and tetrahedra with tensile, bending and volumetric biquadratic springs. Those springs depend on the variation of square edge length while traditional or quadratic springs depend on the change in edge length. However, we establish that for small deformations, biquadratic springs can be approximated with quadratic springs with different stiffnesses. This work leads to an efficient implementation of St Venant-Kirchhoff materials that can cope with compressible strains. It also provides expressions to compute spring stiffnesses on triangular and tetrahedral meshes.

1 Introduction

Surgery simulation requires the real-time modeling of soft tissue deformation. To obtain a viable compromise between realism and computational speed a wide variety of so-called "physically based models" [7] have been developed. For instance mass-spring models are essentially discrete models that define elastic forces between two vertices based on the variation of the edge length. They are still widely used in surgery simulators because they are supposedly both simple to understand and to implement. Those models however cannot be used to discretize properly two or three dimensional elastic materials based on continuum mechanics. Van Gelder [11] showed for instance that spring-mass models cannot represent linear elastic membranes (see section 2.4 for more discussion). The discrete nature of spring-mass systems is particularly problematic when handling unstructured triangular or tetrahedral meshes. To cope with this limitation, a number of researchers [2] have proposed computational methods to estimate the topologies and the stiffness of springs. A common way to cope with this limitation is to define springs on a rectangular [10, 12] lattice in order to improve the isotropy and homogeneity of the deformation.

Several authors have proposed more complex methods than mass-spring models that are to some degree related to continuum mechanics. For instance tensor-mass models [3] correspond to an efficient implementation of linear elastic models while corotational methods [8] extend linear elasticity to large displacements. If those methods are physically plausible they are not hyperelastic materials and are often limited to small deformations. This is why some authors have used also

St Venant Kirchhoff materials for real-time simulation either through optimized data structures [9] or reduced basis [1].

In this paper, we show the *total equivalence* between St Venant Kirchhoff materials defined on discrete surfaces and volumes and a set of *triangular and tetrahedral biquadratic springs*. Those springs do not correspond exactly to the regular springs that are commonly used. However, we show that for small deformations, they are equivalent to regular (quadratic) tensile, angular and volumetric springs, therefore providing analytical expressions of spring stiffness as a function of the rest triangle or tetrahedron geometry. Furthermore, we extend the St Venant Kirchhoff materials to cope with their known limitation in compression. Finally, we show that those biquadratic springs are simple to implement and efficient to compute which makes them well suited for surgery simulation.

2 Membrane Energy on triangular meshes

2.1 Membrane Energy

We consider a two-dimensional compact domain $\Omega \subset \mathbb{R}^2$ being deformed into another domain $\Phi(\Omega)$. A physical point $\mathbf{X} \in \Omega$ is moved to a new position $\Phi(\mathbf{X}) \in \Phi(\Omega)$, the function $\Phi(\mathbf{X})$ being the deformation function. The relative change of length around point \mathbf{X} is captured by a two dimensional tensor, the *right Cauchy-Green deformation tensor* \mathbf{C} , defined as $\mathbf{C} = \nabla\Phi^T \nabla\Phi$ while the deformation is described by the *Green-Lagrange strain tensor* \mathbf{E} : $\mathbf{E} = 1/2(\mathbf{C} - \mathbf{I})$.

With isotropic St Venant Kirchhoff membrane, there exists a linear relationship between the second Piola Kirchhoff stress tensor and the Green-Lagrange strain tensor. The density of membrane energy $W(\mathbf{X})$ can then be written as : $W(\mathbf{X}) = \frac{\lambda}{2}(\text{tr}\mathbf{E})^2 + \frac{\mu}{2}\text{tr}\mathbf{E}^2$ where λ and μ are the Lamé coefficients of the material. Those coefficients are simply related to the physically meaningful Young modulus E and Poisson coefficient ν : $\lambda = \frac{E\nu}{1-\nu^2}$ and $\mu = \frac{E(1-\nu)}{2(1-\nu^2)}$. The Young modulus quantifies the stiffness of the material while the Poisson coefficient characterizes the material compressibility ($\nu = 1.0$ for an incompressible surface material and $\nu = 0.5$ for an incompressible volumetric material).

2.2 Membrane energy of a deformed Triangle

We now consider that the rest surface Ω is discretized as a set of triangles $\{T_i\}, i = \{1, \dots, p\}$ and a set of vertices $\{\mathbf{P}_i\}, i \in \{1, \dots, n\}$. The deformation of that surface is solely determined by the knowledge of the deformed positions of those vertices $\{\mathbf{Q}_i\}, i \in \{1, \dots, n\}$ such that $\mathbf{Q}_i = \Phi_h(\mathbf{P}_i)$. We write as \mathcal{A}_P (resp. \mathcal{A}_Q) the area of the rest triangle T_P (resp. triangle T_Q), l_i (resp. L_i) its edge length and α_i (resp. β_i) its 3 angles (see Figure 1 (Left)).

With a linear triangle element, the deformation function $\Phi(\mathbf{X})$ maps a point $\mathbf{X} \in T_P$ such that $\Phi(\mathbf{X})$ has the same barycentric coordinates in triangle T_Q than \mathbf{X} in triangle T_P :

$$\Phi(\mathbf{X}) = \sum_{i=1}^3 \eta_i(\mathbf{X}) \mathbf{Q}_i = \sum_{i=1}^3 \left(\frac{1}{3} + \mathbf{D}_i \cdot (\mathbf{X} - \mathbf{G}) \right) \mathbf{Q}_i \quad (1)$$

where $\eta_i(\mathbf{X})$ is the barycentric coordinates of \mathbf{X} in T_P , \mathbf{D}_i are the shape vectors of T_P and \mathbf{G} is the centroid of T_P . The shape vectors \mathbf{D}_i are directed along the inner normal (independently of the triangle orientation) and are of length $1/h_i$, h_i being the altitude of \mathbf{P}_i in T_P . They are algebraically defined in 2D as follows :

$$\mathbf{D}_i = \frac{1}{2\mathcal{A}_P}(\mathbf{P}_{i+1} - \mathbf{P}_{i+2})^\perp \quad (2)$$

where $\mathbf{X}^\perp = (-y, x)^T$ is the orthogonal of vector \mathbf{X} .

From this definition of the deformation, one can easily derive the deformation gradient $\nabla\Phi = \left[\frac{\partial\Phi_i}{\partial x_j} \right] = \sum_{i=1}^3 \mathbf{Q}_i \otimes \mathbf{D}_i$ and the trace of the right Cauchy Green tensor $\text{tr}\mathbf{C} = \sum_{i=1}^3 \sum_{j=1}^3 (\mathbf{Q}_i \cdot \mathbf{Q}_j)(\mathbf{D}_i \cdot \mathbf{D}_j)$.

Since C is invariant by translation, one can consider that the origin to be the center \mathbf{O}_Q of the circumscribed circle of T_Q having radius R_Q . Therefore if $i \neq j$, $\mathbf{Q}_i \cdot \mathbf{Q}_j = R_Q^2 - \frac{l_k^2}{2}$ and $\|\mathbf{Q}_i\|^2 = R_Q^2$. Using the property that all shape vectors sum to zero, one gets the following simple expression :

$$\text{tr}\mathbf{C} = - \sum_{i=1}^2 \sum_{j>i}^2 (\mathbf{D}_i \cdot \mathbf{D}_j) l_k^2 = \frac{1}{2\mathcal{A}_P} (l_1^2 \cot \alpha_1 + l_2^2 \cot \alpha_2 + l_3^2 \cot \alpha_3)$$

Finally, by using Heron's formula in triangle T_P which writes the triangle area \mathcal{A}_P as a function of square edge length $\mathcal{A}_P = \frac{1}{4} (L_1^2 \cot \alpha_1 + L_2^2 \cot \alpha_2 + L_3^2 \cot \alpha_3)$ one can formulate the 2 invariants of the strain tensor \mathbf{E} :

$$\text{tr}\mathbf{E} = \frac{\sum_{i=1}^3 \Delta^2 l_i \cot \alpha_i}{2\mathcal{A}_P} \quad \text{tr}\mathbf{E}^2 = \frac{\sum_{i \neq j} 2\Delta^2 l_i \Delta^2 l_j - \sum_{i=1}^3 (\Delta^2 l_i)^2}{64\mathcal{A}_P^2}$$

where $\Delta^2 l_i = (l_i^2 - L_i^2)$ is the square edge elongation.

2.3 Membrane Energy as Triangular Biquadratic Springs

Thus, the total membrane energy to deform triangle T_P into T_Q is a function of square edge variation $\Delta^2 l_i$ and of the angles α_i of the rest triangle :

$$W_{TRBS}(T_P) = \sum_{i=1}^3 \frac{k_i^{TP}}{4} (l_i^2 - L_i^2)^2 + \sum_{i \neq j} \frac{c_k^{TP}}{2} (l_i^2 - L_i^2)(l_j^2 - L_j^2)$$

where k_i^{TP} and c_k^{TP} are the tensile and angular stiffness of the *biquadratic springs* :

$$k_i^{TP} = \frac{2 \cot^2 \alpha_i (\lambda + \mu) + \mu}{16\mathcal{A}_P} \quad c_k^{TP} = \frac{2 \cot \alpha_i \cot \alpha_j (\lambda + \mu) - \mu}{16\mathcal{A}_P}$$

We call this formulation the *TRiangular Biquadratic Springs* (TRBS) since the first term can be interpreted as the energy of three *tensile biquadratic springs* that prevent edges from stretching while the second term can be seen as three *angular*

biquadratic springs that prevent any change in vertex angles (c_k^{TP} controlling the change in angles around \mathbf{Q}_i and \mathbf{Q}_j). Tensile biquadratics springs have a stretching energy which is proportional to the square of the square edge length variation while regular or quadratic springs have an energy related to the edge length variation. The former types of springs are stiffer in extension and looser in compression and are related to the Green-Lagrange strain while the latter are related to the engineering strain [4].

When considering regular triangles, $\alpha_i = \pi/3$, the tensile stiffness is minimal and the angular stiffness is zero for $\nu = 1/3$ and both stiffnesses increase to infinity as ν tends towards 1 (material incompressibility).

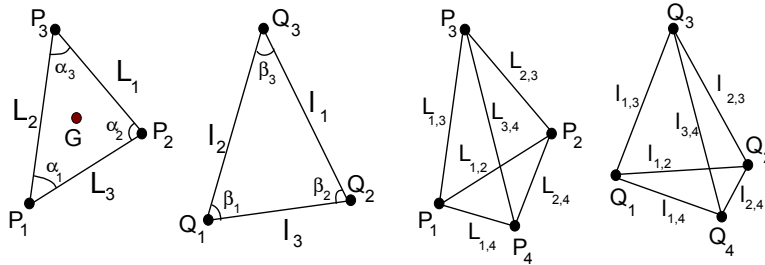


Fig. 1. (Left) Rest triangle T_P having vertices \mathbf{P}_i and its deformed state with vertices \mathbf{Q}_i . (Right) Rest tetrahedron T_P and its deformed state T_Q .

2.4 Small Deformations : Triangular Quadratic Springs

When deformations are small, the square edge elongation $\Delta^2 l_i = (l_i^2 - L_i^2)$ can be simplified as $\Delta^2 l_i \approx 2L_i dl_i$ where $dl_i = l_i - L_i$ is the edge elongation. We define the *TRiangular Quadratic Springs* (TRQS) as an approximation of TRBS :

$$W_{TRQS}(T_P) = \sum_{i=1}^3 \frac{1}{2} \kappa_i^{TP} (dl_i)^2 + \sum_{i \neq j} \gamma_k^{TP} dl_i dl_j$$

where $\kappa_i^{TP} = 4L_i^2 k_i^{TP}$ and $\gamma_k^{TP} = 4L_i L_j c_k^{TP}$ are the corresponding tensile and angular spring stiffnesses.

To the best of our knowledge, it is the first time that a theoretical link between spring-mass models and continuum mechanics is established. Without the addition of angular springs, mass springs models with the right stiffness parameters can at best approximate the behavior of a membrane with $\nu = 1/3$ (see [6] for a similar conclusion based on linear elasticity analogy). With angular springs, the TRQS model is equivalent to the TRBS model but only for small deformations of triangles : $dl_i/L_i < 10\%$.

3 St Venant Kirchoff Elasticity on Tetrahedral Meshes

The elastic energy of a St Venant Kirchoff material is simply expressed as a function of invariant of the Green-Lagrange strain \mathbf{E} : $W^{SVK}(\mathbf{X}) = \frac{\lambda}{2}(\text{tr}\mathbf{E})^2 + \mu \text{tr}\mathbf{E}^2$ where λ and μ are the (volumetric) Lamé coefficients related to Young Modulus and Poisson ratio as follows : $\lambda = \frac{E\nu}{(1+\nu)(1-2\nu)}$ and $\mu = \frac{E}{2(1+\nu)}$.

When discretizing a volumetric body with linear tetrahedral elements, the deformation function $\Phi(\mathbf{X})$ of a tetrahedron \mathcal{T}_P into tetrahedron \mathcal{T}_Q (see Figure 1 (right)) may be written as a function of the barycentric coordinates $\eta_i(\mathbf{X})$ of \mathbf{X} in \mathcal{T}_P similarly to the 2D case. The 4 shape vectors \mathbf{D}_i are then defined as follows :

$$\mathbf{D}_i = (-1)^i \frac{\mathbf{P}_{i+1} \wedge \mathbf{P}_{i+2} + \mathbf{P}_{i+2} \wedge \mathbf{P}_{i+3} + \mathbf{P}_{i+3} \wedge \mathbf{P}_{i+1}}{6\mathcal{V}_P}$$

Following the same approach as in Section 2.2, we can express the first invariant of the strain tensor as:

$$\text{tr}\mathbf{E} = -\frac{1}{2} \sum_{(i,j) \in \mathcal{E}(\mathcal{T})} (\mathbf{D}_i \cdot \mathbf{D}_j) (l_{i,j}^2 - L_{i,j}^2)$$

where $\mathcal{E}(\mathcal{T})$ is the set of 6 edges in tetrahedron \mathcal{T}_P . The expression of the second invariant $\text{tr}\mathbf{E}^2$ is also a function of the variation of square edge length but its complex expression is skipped in this paper due to a lack of space.

From previous results, the total energy to deform tetrahedron \mathcal{T}_P into \mathcal{T}_Q can be derived as a function of square edge variation $\Delta^2 l_i$ and the geometry of the rest tetrahedron :

$$\begin{aligned} W^{TBS}(\mathcal{T}_P) = & \sum_{(i,j) \in \mathcal{E}(\mathcal{T})} \frac{k_{i,j}^{\mathcal{T}_P}}{4} (\Delta^2 l_{i,j})^2 + \sum_{((i,j),(i,k)) \in \mathcal{A}(\mathcal{T})} \frac{c_{[i],[j],[k]}^{\mathcal{T}_P}}{2} \Delta^2 l_{i,j} \Delta^2 l_{i,k} + \\ & \sum_{((i,j),(k,l)) \in \mathcal{O}(\mathcal{T})} \frac{d_{[i],[j],[k],[l]}^{\mathcal{T}_P}}{2} \Delta^2 l_{i,j} \Delta^2 l_{k,l} \end{aligned}$$

– $k_{i,j}^{\mathcal{T}_P}$ is a tensile stiffness of a spring linking vertex i and j .

$$k_{i,j}^{\mathcal{T}_P} = \frac{(\lambda + \mu)\mathcal{V}_P}{2} (\mathbf{D}_i \cdot \mathbf{D}_j)^2 + \frac{\mu^* \mathcal{V}_P}{2} \|\mathbf{D}_i\|^2 \|\mathbf{D}_j\|^2$$

– $c_{[i],[j],[k]}^{\mathcal{T}_P}$ is an angular stiffness that prevents the triangle linking vertices i , j and k from changing its angle around vertices j and k . $\mathcal{A}(\mathcal{T})$ is the set of 12 adjacent pair of edges (edge pairs having one and only one vertex in common) in \mathcal{T}_P .

$$c_{[i],[j],[k]}^{\mathcal{T}_P} = \frac{(\lambda + \mu)\mathcal{V}_P}{2} (\mathbf{D}_i \cdot \mathbf{D}_j)(\mathbf{D}_i \cdot \mathbf{D}_k) + \frac{\mu\mathcal{V}_P}{2} \|\mathbf{D}_i\|^2 (\mathbf{D}_j \cdot \mathbf{D}_k)$$

– $d_{[i,j],[k,l]}^{\mathcal{T}_P}$ is a volumetric stiffness that prevents the tetrahedron \mathcal{T}_P from collapsing. $\mathcal{O}(\mathcal{T})$ is the set of 3 opposite pair of edges in \mathcal{T}_P .

$$d_{[i,j],[k,l]}^{\mathcal{T}_P} = \frac{\lambda \mathcal{V}_P}{2} (\mathbf{D}_i \cdot \mathbf{D}_j)(\mathbf{D}_k \cdot \mathbf{D}_l) + \frac{\mu \mathcal{V}_P}{2} ((\mathbf{D}_i \cdot \mathbf{D}_k)(\mathbf{D}_j \cdot \mathbf{D}_l) + (\mathbf{D}_i \cdot \mathbf{D}_l)(\mathbf{D}_j \cdot \mathbf{D}_k))$$

Thus the elastic energy can be decomposed into the sum of $6 + 12 + 3 = 21$ terms. We call this formulation of the St Venant Kirchoff energy, the *Tetrahedral Biquadratic Springs* (TBS).

Similarly to the membrane energy, each biquadratic springs may be approximated by a quadratic spring by making the following hypothesis : $\Delta^2 l_{i,j} \approx 2L_{i,j}(l_{i,j} - L_{i,j}) = 2L_{i,j} dl_{i,j}$. Typically those approximations are valid for small strains, *i.e.* when $|dl_{i,j}/L_{i,j}| < 0.1$. Under this hypothesis, we can define the *Tetrahedral Quadratic Springs* (TQS) as an approximation of TBS :

$$W^{TQS}(\mathcal{T}_P) = \sum_{(i,j) \in \mathcal{E}(\mathcal{T})} \frac{\chi_{i,j}^{\mathcal{T}_P}}{4} (dl_{i,j})^2 + \sum_{((i,j),(i,k)) \in \mathcal{A}(\mathcal{T})} \frac{\gamma_{[i],[j],[k]}^{\mathcal{T}_P}}{2} dl_{i,j} dl_{i,k} + \sum_{((i,j),(k,l)) \in \mathcal{O}(\mathcal{T})} \frac{\xi_{[i,j],[k,l]}^{\mathcal{T}_P}}{2} dl_{i,j} dl_{k,l}$$

where the TQS tensile, angular and volumetric stiffnesses are proportional to their TBS counterpart :

$$\chi_{i,j}^{\mathcal{T}_P} = 4L_{i,j}^2 k_i^{\mathcal{T}_P} \quad \gamma_{[i],[j],[k]}^{\mathcal{T}_P} = 4L_{i,j}L_{i,k} c_{[i],[j],[k]}^{\mathcal{T}_P} \quad \xi_{[i,j],[k,l]}^{\mathcal{T}_P} = 4L_{i,j}L_{k,l} c_{[i,j],[k,l]}^{\mathcal{T}_P}$$

4 Compressible St Venant Kirchhoff Materials

The elastic energy of St Venant Kirchhoff material only depends on the invariants of \mathbf{E} which implies that this elastic energy is invariant with respect to any rotations, translations but also any plane reflexion. Therefore, it is easy to show that the elastic energy becomes locally minimum when a triangle or tetrahedron becomes flat. This entails that zero elastic force is applied to resist the collapse of a triangle or tetrahedron. This severely limits the use of St Venant Kirchhoff materials since it is not appropriate to simulate materials under compression.

There exists different ways to cope with this limitation. If $J = \det \Phi$ is the ratio of the deformed volume over the rest volume, then one option is to add an energy term proportional to $(J - 1)^2$ [9] or to $\log |J|$ as done for Neo Hookean materials. Also some authors have proposed to cope for flat or inverted elements at the cost diagonalizing the deformation gradient matrix with a polar [5] or QR [8] decomposition .

In order to improve the compressibility of St Venant Kirchhoff (SVK) materials while limiting the added computational cost, we propose to add the following energy W^{comp} term to the energy : $W^{comp} = 0$ if $J > 1$ and $W^{comp} = (\lambda + \mu)(J - 1)^4/2$ if $J < 1$. Figure 2 (Left) compares the elastic force on a single tetrahedron when a vertex is moved toward its opposite triangle, F^{SVK} being

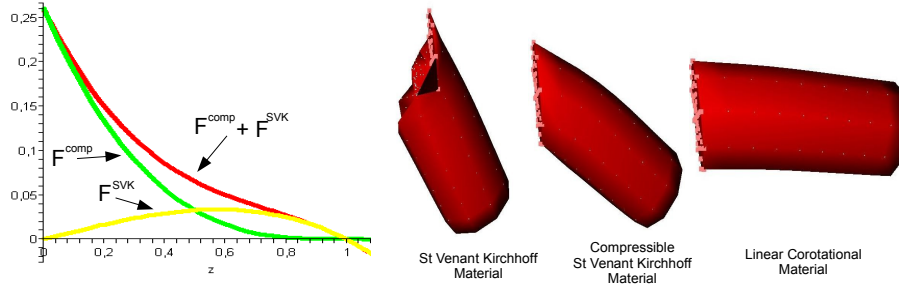


Fig. 2. (Left) Effect of the added volume penalty term F^{comp} on the compression force computed on a single tetrahedron; (Right) Compressible constraint allows to compute the large bending of cylinder under its own weight.

the regular SVK force and F^{comp} being the additional force. The composite force $F^{comp} + F^{SVK}$ is C^1 continuous and is a cubic function of strain similarly to the extension case. Compression strain of more than 50% can be reached with this formulation. Figure 2 (Right) shows the effect of the additional compression energy on a soft cylinder clamped on one side and bending upon its own weight. With the regular SVK material, several tetrahedra collapse due to the amount of compression (thus falling into a local minimum) but not for the compressible SVK. Furthermore, the compressible SVK bends significantly but much less than a corotational material having the same Lamé coefficients ($E = 1$, $\nu = 0.35$). This shows that corotational models have a far greater resistance to shear stress than SVK models.

5 Results and Implementation issues

In this paper, we provide analytical stiffness parameters $\kappa_{i,j}^{TP}$ and $\chi_{i,j}^{TP}$ involving Young Modulus and Poisson ratios for spring mass-models defined on triangulation and tetrahedral meshes. We have verified that those spring-mass models behave consistently whether the mesh is regularly tessellated or not [4]. Their behavior is however physically plausible only on triangulations for a choice of the Poisson coefficient equal to 1/3. To obtain reasonable results for other Poisson coefficient, it is required to implement the full TRQS and TQS models that involve angular and volumetric springs.

The TBS, TQS, TRBS and TRQS models have been implemented in the SOFA platform, elastic force and tangent stiffness matrices being analytically derived from the elastic energy presented in this paper. In terms of performance, preliminary studies show that the TBS and TRBS are slightly faster than the TRQS and TQS, since the former do not involve any square root evaluation and lead to simpler expression. Figure 3 (Top) provides some benchmark for the elastic force evaluation and stiffness matrix-vector product on a triangulation computed on a laptop computer with a Core Duo T2400 1.83 MHz processor.

In this implementation, edges, triangles and tetrahedra are successively scanned to apply respectively tensile, angular and volumetric forces. It appears that the biquadratic model is only 60% more expensive than the spring-mass model, while the quadratic model is itself 60 % more expensive than the biquadratic model. On tetrahedral meshes, first implementations seem to indicate similar trends, with the TQS model being twice slower than the TBS, and in the worst case (when all tetrahedra are compressed) the compressible TBS being 65% slower than the regular TBS model. Corotational models seem also be 80% slower than the regular TBS. Figure 3 (Bottom) show the use of a compressible TBS model for surgery simulation on a tetrahedral mesh with 1059 vertices and 5015 tetrahedra. Interactive simulation of resection was obtained using an implicit Euler time integration. Edge, triangle and tetrahedra stiffnesses are updated each time tetrahedra are being removed.

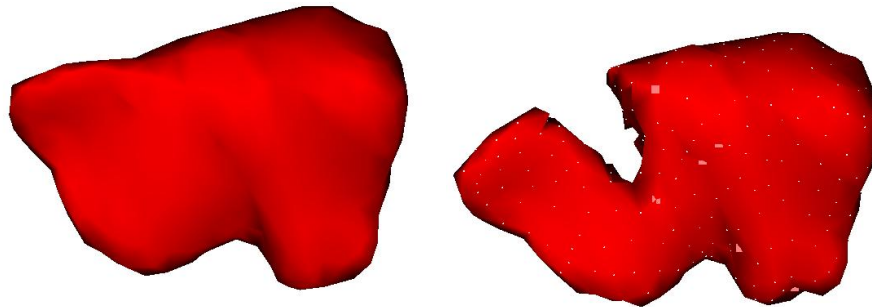
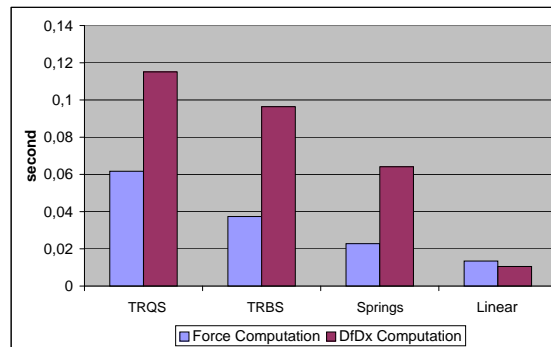


Fig. 3. (Top) Execution times of the elastic force and the matrix-vector product for 4 different elastic membrane formulations; (Bottom) Liver surgery simulation performed in real time with a compressible TBS model before and after resection.

6 Conclusion

In this paper, we have first showed the equivalence between surface and volumetric St Venant Kirchhoff materials and triangular and tetrahedral biquadratic springs. Furthermore we showed that quadratic tensile, angular and volumetric spring models correspond to small deformations approximations of those biquadratic springs. Finally we have improved the compression behavior of the St Venant Kirchhoff material by adding a volume penalty which makes the compression and extension forces symmetric.

Future work should include a more thorough comparison with existing FEM or corotational methods both in terms of computational performance and behavior. Extension of the proposed approach to anisotropic and incompressible materials is also important to produce realistic soft tissue deformation.

References

1. J. Barbič and D. L. James. Real-time subspace integration for St. Venant-Kirchhoff deformable models. *ACM TOG (SIGGRAPH 2005)*, 24(3):982–990, Aug. 2005.
2. G. Bianchi, B. Solenthaler, G. Székely, and M. Harders. Simultaneous topology and stiffness identification for mass-spring models based on fem reference deformations. In C. Barillot, editor, *Medical Image Computing and Computer-Assisted Intervention MICCAI 2004*, volume 2, pages 293–301. Springer, November 2004.
3. S. Cotin, H. Delingette, and N. Ayache. A hybrid elastic model allowing real-time cutting, deformations and force-feedback for surgery training and simulation. *The Visual Computer*, 16(8):437–452, 2000.
4. H. Delingette. Triangular springs for modeling nonlinear membranes. *IEEE Transactions on Visualization and Computer Graphics*, 14(2):329–341, March/April 2008.
5. G. Irving, J. Teran, and R. Fedkiw. Tetrahedral and hexahedral invertible finite elements. *Graph. Models*, 68(2):66–89, 2006.
6. B. Lloyd, G. Székely, and M. Harders. Identification of spring parameters for deformable object simulation. *IEEE Transactions on Visualization and Computer Graphics*, 13(5):1081–1094, Sept.-Oct. 2007.
7. A. Nealen, M. Muller, R. Keiser, E. Boxerman, and M. Carlson. Physically based deformable models in computer graphics. Technical report, Eurographics State of the Art, Dublin, Ireland, Sept. 2005.
8. M. Nesme, Y. Payan, and F. Faure. Efficient, physically plausible finite elements. In J. Dingliana and F. Ganovelli, editors, *Eurographics (short papers)*, august 2005.
9. G. Picinbono, H. Delingette, and N. Ayache. Non-Linear Anisotropic Elasticity for Real-Time Surgery Simulation. *Graphical Models*, 65(5):305–321, Sept. 2003.
10. D. Terzopoulos, J. Platt, A. Barr, and K. Fleischer. Elastically deformable models. In *Computer Graphics (SIGGRAPH-87)*, volume 21, pages 205–214, 1987.
11. A. Van Gelder. Approximate simulation of elastic membranes by triangulated spring meshes. *Journal of Graphics Tools: JGT*, 3(2):21–41, 1998.
12. K. Waters and D. Terzopoulos. Modeling and animating faces using scanned data. *The Journal of Visualization and Computer Animation*, 2:129–131, 1991.